

Transition radiation of electrons with orbital angular momentum

A. S. Konkov¹⁾, A. P. Potylitsyn, M. S. Polonskaya

Tomsk Polytechnic University, 634050 Tomsk, Russia

Submitted 12 August 2014

Several experimental groups have recently obtained the so-called vortex electrons (electrons with orbital angular momentum (OAM) of $\ell \leq 100\hbar$) with energies of ~ 300 keV. The angular momentum of such electrons becomes proportional to the OAM value, which leads to the corresponding increase of the electron magnetic moment. In this paper, we investigate the transition radiation from the “charge + magnetic moment” system by means of the classical electrodynamics theory. The circular polarization of optical transition radiation reaches its maximum level to $\sim 70\%$, which allows to use this effect for the independent measurement of the electron orbital momentum value.

DOI: 10.7868/S0370274X14190011

1. Introduction. Beams of vortex particles are basically the beams with phase singularity, which consist in the intensity absence and the wavefront phase ambiguity in the center of this beam [1]. Wavefront of such particles has the form of a spiral, and a wave phase can be changed from 0 to 2π multiply to ℓ . In this case ℓ characterizes the strength of “vortex” and is called a topological charge or the orbital angular momentum (OAM). The “vortex effect” is achieved by overlapping of separate particles wavefronts in such a way that at each point of space the local wave directions are twisted relative to the preferred axis (for example, relative to the mean momentum of the wave).

The existence of vortex photon beams was theoretically predicted in the paper [2] more than 20 years ago. In this paper was considered the transformation of laser beams with a high-order Laguerre–Gaussian mode into the beams with a high-order Hermite–Gaussian mode. In the result of such transformation the photons get OAM, which can be measured mechanically. The study of vortex electrons started a bit later with the fundamental paper [3]. In this paper was demonstrated the occurrence of the free electron beams with OAM from the Schrödinger equation solution for paraxial wave packets with a vortex phase and found the connection between OAM and magnetic moment for such particles.

Authors of recent experiments [4–6] have been obtained the vortex electrons beams with the OAM value up to $\ell \sim 100\hbar$. Direct measurement of the OAM value which carried by electrons can be performed to determine the mechanical moment transferred to a target if electrons are totally absorbed in it. However, unlike with analogue measurements with the OAM photon beam,

the electrons absorption in a target is connected with non-uniform energy deposition along both the beam profile and the target depth, which will introduce noticeable errors during the OAM measurements.

The optical measurements accuracy being several orders higher than that of mechanical measurements, it seems undoubtedly promising to determine the possibility of the OAM electrons value by its radiation characteristics. The main radiation mechanisms of non-relativistic electrons are transition radiation (TR) and bremsstrahlung [7]. Both mechanisms have already been studied in details in a theoretical point of view and experimentally, as well. The authors of the paper [8] have shown that OAM summarizes with the intrinsic electron magnetic moment, which leads to the increase of resultant magnetic moment that is ℓ times greater than the Bohr magneton $\mu_B = e\hbar/2m_e c$. As shown in [6], a beam of electrons with OAM that is parallel or antiparallel to a momentum can be formed by spatial selection. Because if in this case the orbital momentum $\ell = \ell \mathbf{e}_p$ (where \mathbf{e}_p is the unit momentum vector) quantization axis is determined for electron beams with OAM (it coincides with averaged electron beam momentum \mathbf{p}), the same quantization axis can be used for the electron magnetic moment $\boldsymbol{\mu} = g\mu_B \ell$ (where g is the gyromagnetic ratio) and one can consider the so-called longitudinal magnetic moment orientation.

As it is well-known that the bremsstrahlung intensity in the range of photon frequency $\omega < \gamma\omega_p$ (where γ is the electron Lorentz factor, ω_p is the plasma frequency of target material) is significantly suppressed in comparison with TR. In the case of non-relativistic electrons ($\gamma \sim 1$), the optical TR process is more preferable for the investigation of vortex electrons radiation characteristics, because of condition $\hbar\omega_{\text{opt}} < \hbar\omega_p$, the TR inten-

¹⁾e-mail: Ekwinus@tpu.ru

sity is significantly higher than of bremsstrahlung. It is observed in the paper [9] the optical TR characteristics of electrons with kinetic energy as small as $E_k = 80$ keV.

2. Transition radiation fields. In the case of electrons with magnetic moment or OAM, TR will not only be generated by the charge, but by a magnetic moment as well. Having considered the spatial parity of the scalar value that characterize the TR process of longitudinal magnetic moment $\boldsymbol{\mu}$ can be presented as a mixed vector product that is characterized the TR circular polarization:

$$\boldsymbol{\mu}[\mathbf{b}, \mathbf{k}], \quad (1)$$

where \mathbf{k} is the photon momentum, \mathbf{b} is a vector perpendicular to the target interface. It is obvious that for perpendicular electron beam incident on the target (vacuum-medium interface) the expression (1) is equal to zero. However, the circularly polarized radiation component appears under the oblique electron incident with magnetic moment $\boldsymbol{\mu}$ on the target of non-coplanar geometry (vector \mathbf{k} lies out of the plane $(\boldsymbol{\mu} \cdot \mathbf{b})$, see Fig. 1).

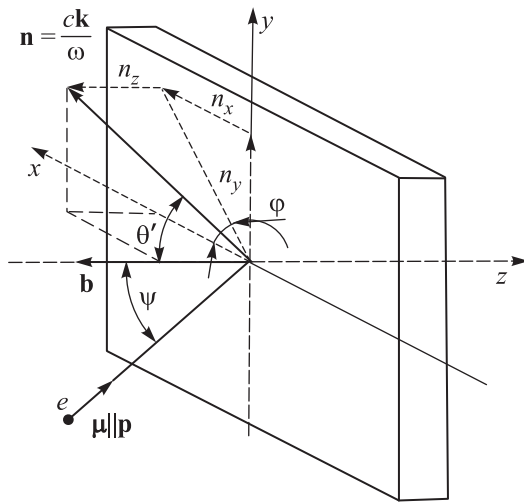


Fig. 1. Scheme of TR generation for oblique electron incident on the target

For magnetic moment values $|\boldsymbol{\mu}| \gg \mu_B$, TR of the “charge + magnetic moment” system can be considered according to the classical approach with a good accuracy as in the book [10], where was only investigated the perpendicular passage through the border of two interfaces, in the case when the TR circular polarization is absent and, hence, is not considered. In the paper [11], it were obtained the expressions for resulting TR field of the “charge + magnetic moment” system directed into the back-hemisphere (around the specular reflection direction – “backward TR”) for oblique electron incident on

the target with permittivity $\varepsilon = \varepsilon' + i\varepsilon''$. To obtain the results, it was used the images method [12] that allows to obtain the TR characteristics for any geometry.

For an ideally conducting target ($|\varepsilon''| \rightarrow \infty$), the fields in the reference frame that is shown in the Fig. 1 are as follows:

$$E_x = C_1 \left\{ e\beta_z n_x n_z + i\gamma^{-1} \frac{\omega}{c} \mu \left[B_z(1 - \beta_y n_y) n_y - \right. \right. \quad (2)$$

$$\left. \left. - \beta_z n_z^2 B_y \right] \right\},$$

$$E_y = C_1 \left\{ e\beta_z \left[n_y n_z - \beta_y n_z \right] + i\gamma^{-1} \frac{\omega}{c} \mu \left[\beta_z n_z^2 B_x - \right. \quad (3)$$

$$\left. - B_z(1 - \beta_y n_y) n_x \right] \right\},$$

$$E_z = C_1 \left\{ e\beta_z \left[n_z^2 - 1 + \beta_y n_y \right] + \quad (4)$$

$$+ i\gamma^{-1} \frac{\omega}{c} \mu \beta_z n_z \left[B_y n_x - B_x n_y \right] \right\}.$$

Here e is the electron charge, μ is the magnetic moment,

$$\mathbf{n} = \mathbf{k}c/\omega = \{\sin \theta' \cos \phi, \sin \theta' \sin \phi, \cos \theta'\},$$

$$\boldsymbol{\beta} = \{0, \beta_y, \beta_z\} = \beta\{0, \sin \psi, \cos \psi\},$$

$$B_x = n_y \cos \psi - (\gamma\beta)^{-1} \sin \psi,$$

$$B_y = n_x (\gamma \sin^2 \psi - \cos^2 \psi),$$

$$B_z = n_x (1 + \gamma) \sin \psi \cos \psi,$$

$$C_1 = \frac{\exp(i\omega R/c)}{\pi c R [(1 - \beta_y n_y)^2 - \beta_z^2 n_z^2]}.$$

The TR field components (2)–(4) were obtained by the images method according to the paper [11] using the known relations for the connection of electric force vector with Hertz potentials, both for electric charge and magnetic moment (see, for example [13]). A real component of the field describes TR of electric charge, while an imaginary part of the radiation field corresponds to magnetic moment. Terms B_i , contained in the formulae (2)–(4), characterize the angular components of the current density, induced by the particle magnetic moment. Common multiplier C_1 includes a term, describing a spherical wave with frequency ω at distance R from the target. It should be noted, that the polar angle θ' , included in the expression for the unit wave vector \mathbf{n} , is measured from the negative direction of z axis and is connected with a polar angle θ by a simple relation: $\theta' = \pi - \theta$.

3. Stokes parameter for transition radiation.

In order to calculate the circular polarization degree (Stokes parameter ξ_3), one needs to use the field components defined in a plane perpendicular to the photon momentum \mathbf{k} [14]:

$$\xi_3 = i \frac{E_1^* E_2 - E_1 E_2^*}{|E_1|^2 + |E_2|^2}. \quad (5)$$

For this in the formula (5) the radiation field components E_1, E_2 are defined in the reference frame with unit polarization vectors $\mathbf{e}_1, \mathbf{e}_2$ [7]:

$$\mathbf{e}_1 = \frac{[\mathbf{n}, \mathbf{b}]}{|[\mathbf{n}, \mathbf{b}]|} = \frac{\{-n_y; n_x; 0\}}{\sqrt{1 - n_z^2}}, \quad (6)$$

$$\mathbf{e}_2 = [\mathbf{n}, \mathbf{e}_1] = \frac{\{-n_x n_z; -n_y n_z; 1 - n_z^2\}}{\sqrt{1 - n_z^2}}. \quad (7)$$

After simple transformations one can get:

$$E_i = (\mathbf{E} \mathbf{e}_i) = \frac{C_1}{\sqrt{1 - n_z^2}} \left(e E_{ei} + i \frac{\omega}{\gamma c} \mu E_{\mu i} \right), \quad (8)$$

where all values of $E_{e,\mu,i}$ are real:

$$\begin{aligned} E_{e1} &= -\beta_y \beta_z n_x n_z, & E_{e2} &= -\beta_z (1 - \beta_y n_y - n_z^2), \\ E_{\mu 1} &= \beta_z n_z^2 (B_x n_x + B_y n_y) - B_z (1 - \beta_y n_y) (1 - n_z^2), \\ E_{\mu 2} &= \beta_z n_z (B_y n_x - B_x n_y). \end{aligned}$$

For the geometry under consideration the denominator in (5) is expressed as follows:

$$\begin{aligned} |E_1|^2 + |E_2|^2 &= \frac{|C_1|^2}{1 - n_z^2} \left(e^2 \beta_z^2 \left[\beta_y^2 n_x^2 n_z^2 + \right. \right. \\ &+ (1 - \beta_y n_y - n_z^2)^2 \left. \right] + \frac{\omega^2}{\gamma^2 c^2} \mu^2 \cos^2 \psi \left\{ n_x^2 \left[\sin \psi \times \right. \right. \\ &\times (1 + \gamma) (1 - \beta_y n_y - n_z^2) + \gamma^{-1} n_z^2 \sin \psi + \\ &+ \beta n_z^2 n_y (1 - \cos \psi) \left. \right]^2 + n_z^2 \left[\gamma \beta_y n_x^2 \sin \psi - \right. \\ &\left. \left. - \beta_z n_x^2 \cos \psi - \beta_z n_y^2 + \gamma^{-1} n_y \sin \psi \right]^2 \right\} \right). \quad (9) \end{aligned}$$

As expected, the expression (9), describing the TR intensity, is a sum of two terms: the former is proportional to the charge squared and describes the ordinary TR, and the latter, which is proportional to the magnetic moment squared, describes the radiation of the longitudinal magnetic moment. The intensity of the longitudinal magnetic moment radiation does not depend on its orientation (parallel or antiparallel to the momentum \mathbf{p}). The expression (9) coincides with the results from [10, 15] in the limiting case of perpendicular passage ($\psi = 0$) on the condition that $e = 0$.

Let's consider radiation in the plane of particle incidence ($n_x = 0$) when direction cosines n_y, n_z are expressed only through the polar angle θ' : $n_y = \sin \theta'$, $n_z = \cos \theta'$. In this case a denominator in the formula (9) (see expression for C_1) can be written in the following form:

$$\begin{aligned} &\left[1 - \beta (\sin \psi \sin \theta' - \cos \psi \cos \theta') \right]^2 \times \\ &\times \left[1 - \beta (\sin \psi \sin \theta' + \cos \psi \cos \theta') \right]^2 = \\ &= \left[1 - \beta \cos(\psi - \theta') \right]^2 \left[1 + \beta \cos(\psi + \theta') \right]^2. \end{aligned}$$

As $0 < \theta' \leq \pi/2$, then radiation maximum values in the plane of incidence ($\phi = \pi/2$) are determined from the following condition:

$$\sin \theta' = \beta \sin \psi \pm \beta^{-1} \sqrt{(1 - \beta^2)(1 - \beta^2 \sin^2 \psi)}.$$

Radiation angles which obey a condition $\sin \theta' = \beta \sin \psi$, correspond to the minimum in TR spectral-angular distribution. For relativistic electrons the TR spectral-angular distribution becomes a symmetrical lobe-shaped with a minimum in a mirror reflection direction with two maxima that are situated at angles $\theta' \sim \gamma^{-1}$ relatively to mirror reflection direction. With the decrease of electron energy the distribution takes an asymmetrical form and is greatly expanded. TR of electric charge is linearly polarized, but due to the magnetic moment contribution under oblique incidence in the minimum domain of TR a circular polarized component occurs.

The numerator in (5) is defined in the same way:

$$\begin{aligned} i (E_1^* E_2 - E_1 E_2^*) &= 2 |C_1|^2 \frac{\omega}{\gamma c} \frac{e \mu \beta_y n_x \cos \psi}{(1 - n_z^2)} \times \\ &\times \left(\beta_z n_z (\gamma \beta_y n_x^2 \sin \psi - \beta_z n_x^2 \cos \psi - \beta_z n_y^2 + \gamma^{-1} n_y \sin \psi) + \right. \\ &+ (1 - \beta_y n_y - n_z^2) \left\{ n_z^2 [\gamma^{-1} \cos \psi + \beta n_y \cot \psi (1 - \cos \psi)] + \right. \\ &\left. \left. + (1 + \gamma) (1 - \beta_y n_y - n_z^2) \cos \psi \right\} \right). \quad (10) \end{aligned}$$

It is noteworthy that the factor $\mu \beta_y n_x$ in the numerator (10) just corresponds to the mixed product

$$(\boldsymbol{\mu} | \mathbf{b}, \mathbf{n}) = \frac{\mu}{\beta} (\boldsymbol{\beta} | \mathbf{b}, \mathbf{n}). \quad (11)$$

4. Discussion. Figure 2 shows the TR angular distributions for a perfectly conducting target and incident angles $\psi = \pi/4$ and $\pi/3$ for kinetic electron energy $E_k = 300$ keV ($\gamma = 1.587$) for two photon energies $\hbar\omega_1 = 2$ eV and $\hbar\omega_2 = 1$ eV. The existence of radiation defined by a magnetic moment leads to the distribution, when the minimum in the radiation intensity will be non-zero (unlike the ordinary TR). For a perfectly conducting target, the ordinary TR characteristics do not depend on the energy of photons that are emitted. For the TR from a magnetic moment, there is a dependence on frequency (see the second summand in (9)); however the Bohr magneton radiation intensity is $(\hbar\omega/\gamma m_e c^2)^2$ times smaller than the TR intensity of charge [11], so the total intensity virtually does not depend on the frequency.

Figure 3 shows the dependence of Stokes parameter ξ_3 on polar and azimuthal angles of emission the TR

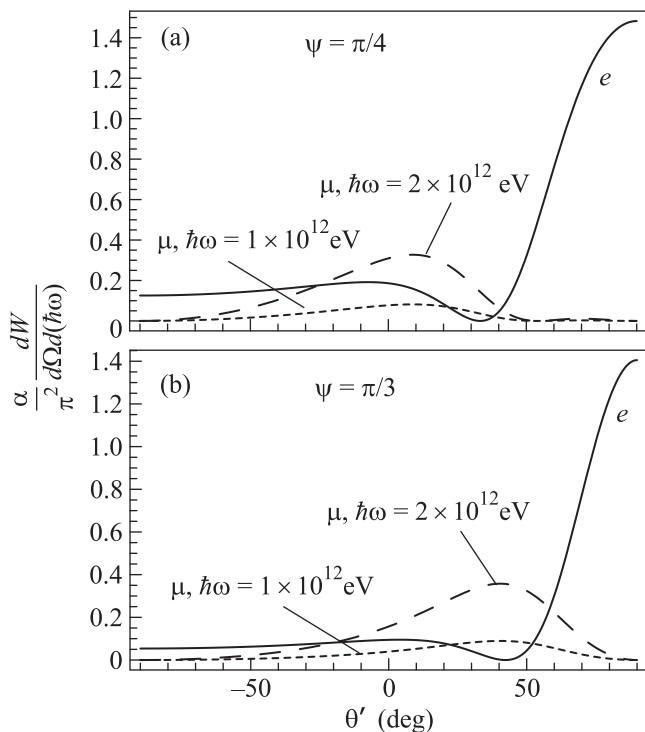


Fig. 2. TR angular distribution for electrons with energy $E_k = 300$ keV from a perfectly conducting target on the conditions that $\mu = \mu_B$ and $\phi = \pi/2$ (the intensity of the magnetic moment TR is depicted 10^{12} times higher for convinence). The solid line represents the ordinary TR defined by a charge; the dashed line, the magnetic moment TR for the photons with energy $\hbar\omega_1 = 2$ eV; the dotted line, the magnetic moment TR for the photons with energy $\hbar\omega_2 = 1$ eV

photons with the same energy. The calculations were performed for the target tilt angle $\psi = \pi/3$, since in this case the valley region of the TR is close to $\theta' = 45^\circ$, which leads to the increase of expression (1).

As one can see in the Fig. 4, circular polarization does not exceed 1% for the TR of a longitudinally spin-polarized electron. However, this value increases significantly for electrons with OAM ($\ell \gg \hbar$) (see Fig. 3). The circular polarization degree is linearly dependent on OAM value only by small ℓ and photon energies. An increase of emitted radiation energy shows more obvious contribution from the second term in the expression (9), that leads to the breaking of the linear dependence of Stokes parameter ξ_3 on OAM value ℓ .

It should be mentioned that in the region of minimum radiation intensity (near $\theta' = 42.26^\circ$, see Fig. 2b) the radiation circular polarization for electrons with $\ell \approx 100\hbar$ can reach the values to 70% in dependence on radiation angles (see Fig. 3).

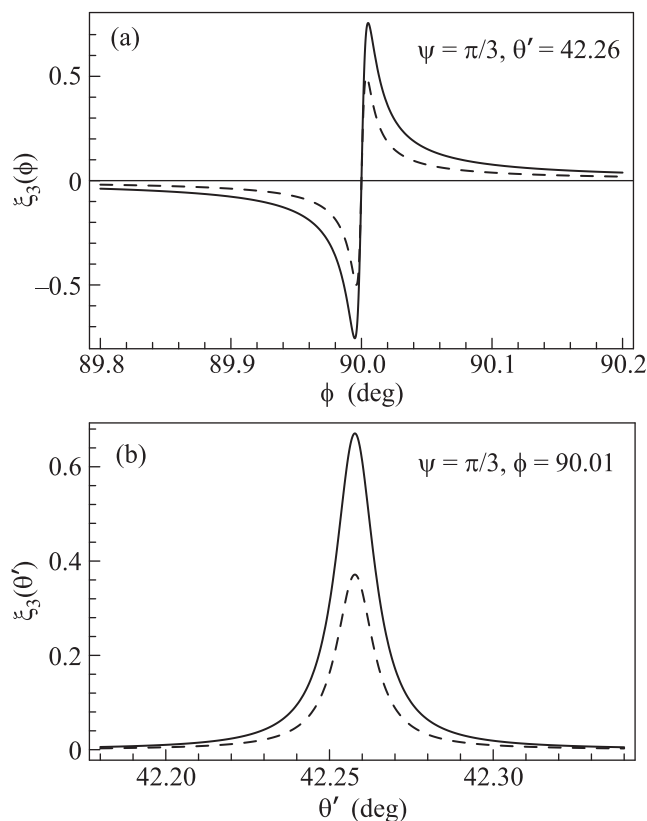


Fig. 3. Dependence of Stokes parameter ξ_3 on polar θ' and azimuthal ϕ angles of TR with photon energies $\hbar\omega_1 = 2$ eV (solid line) and $\hbar\omega_2 = 1$ eV (dashed line) from perfectly conducting target for $\mu = 100\mu_B$

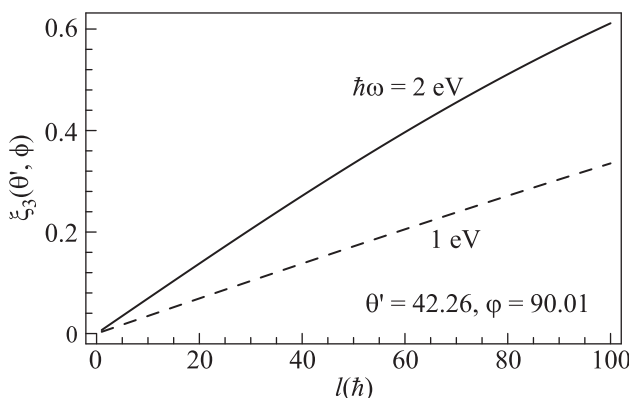


Fig. 4. Stokes parameter ξ_3 as a function of OAM value ℓ for the case of the target tilt angle $\psi = \pi/3$

5. Summary and conclusions. Hence, one can measure the OAM value by measuring the circular polarization of optical TR from electrons with OAM in the range of the angles that correspond to the minimum TR intensity. In this case the accuracy of such optical measurements could be better than 1%. However, for such measurements are needed very sensitive detectors

because the total yield of circularly polarized radiation reaches values of 2–10 photons per second in the energy range from 1 to 5 eV with a beam current of 1 nA.

The TR characteristics for polished aluminum in the optical region are close to the calculated ones for perfect conductor [16, 17]. Therefore, the evaluations obtained hereinabove are expected to be valid for a polished metal target.

In the paper [18] is shown that the quantum consideration of the Bohr magneton TR intensity gives some enhancement in comparison with calculations using classical electrodynamics. But if magnetic moment is about ~ 100 times exceeds the Bohr magneton, one should expect that the quantum corrections will be insignificant.

Authors are grateful to V.G. Serbo, I.P. Ivanov, and D.V. Karlovets for stimulating criticism and useful discussions. The work was partially supported by Russian Ministry of Science and Education within the grants # 14.B37.21.0912 and 0.339.2012.

1. J. F. Nye and M. V. Berry, Proc. R. Soc. Lond. A **336**, 165 (1974).
2. L. Allen, M. W. Beijersbergen, R. J. C. Spreeuw, and J. P. Woerdman, Phys. Rev. A **45**, 8185 (1992).
3. K. Y. Bliokh, Y. P. Bliokh, S. Savel'ev, and F. Nori, Phys. Rev. Lett. **99**, 190404 (2007).
4. M. Uchida and A. Tonomura, Nature **464**, 737 (2010).
5. J. Verbeeck, H. Tian, and P. Schattschneider, Nature **467**, 301 (2010).
6. B. J. McMorran, A. Agrawal, I. M. Anderson, A. A. Herzing, H. J. Lezec, J. J. McClelland, and J. Unguris, Science **331**, 192 (2011).
7. A. P. Potylitsyn, *Electromagnetic Radiation of Electrons in Periodic Structures*, Springer, Berlin (2011).
8. K. Y. Bliokh, M. R. Dennis, and F. Nori, Phys. Rev. Lett. **107**, 174802 (2011).
9. C. Bal, E. Bravin, E. Chevallay, T. Lefèvre, and G. Suberlucq, *Proc. DIPAC 2003 – Mainz, Germany*, v. PM04.
10. V. L. Ginzburg and V. N. Tsytovich, *Transition Radiation and Transition Scattering*, A. Hilger, Bristol (1990).
11. A. S. Konkov, A. P. Potylitsyn, and V. A. Serdutskiy, Russ. Phys. J. **54**, 1249 (2012).
12. V. E. Pafomov, Proc. FIAN USSR **44**, 90 (1969).
13. J. D. Jackson, *Classical Electrodynamics*, Wiley, N.Y. (1962).
14. E. Collett, *Field Guide to Polarization*, SPIE, Washington (2005).
15. M. Sakuda, Phys. Rev. Lett. **72**, 804 (1994).
16. L. Wartski, S. Roland, J. Lasalle, M. Bolore, and G. Filippi, J. Appl. Phys. **46**, 3644 (1975).
17. A. P. Potylitsyn, Nucl. Instr. and Meth. B **145**, 169 (1998).
18. M. Sakuda and Y. Kurihara, Phys. Rev. Lett. **74**, 1284 (1995).